Inorg. Chem. **2007**, *46*, 5411–5418

Table Salt and Other Alkali Metal Chloride Oligomers: Structure, Stability, and Bonding

F. Matthias Bickelhaupt,*,† Miquel Solà,*,‡ and Célia Fonseca Guerra†

Afdeling Theoretische Chemie, Scheikundig Laboratorium der Vrije Universiteit, De Boelelaan 1083, NL-1081 HV Amsterdam, The Netherlands, and Institut de Química Computacional, Universitat de Girona, Campus Montilivi, E-17071 Girona, Catalonia, Spain

Received February 20, 2007

We have investigated table salt and other alkali metal chloride monomers, ClM, and (distorted) cubic tetramers, $(ClM)_4$, with M = Li, Na, K, and Rb, using density functional theory (DFT) at the BP86/TZ2P level. Our objectives are to determine how the structure and thermochemistry (e.g., Cl–M bond lengths and strengths, oligomerization energies, etc.) of alkali metal chlorides depend on the metal atom and to understand the emerging trends in terms of quantitative Kohn–Sham molecular orbital (KS-MO) theory. The analyses confirm the high polarity of the Cl–M bond (dipole moment, VDD, and Hirshfeld atomic charges). They also reveal that bond overlap derived stabilization (approximately –26, –20, and –8 kcal/mol), although clearly larger than in the corresponding F–M bonds, contributes relatively little to the (trend in) bond strengths (–105, –90, and –94 kcal/mol) along M = Li, Na, and K. Thus, the Cl–M bonding mechanism resembles more closely that of the even more ionic F–M bond than that of the more covalent C–M or H–M bonds. Tetramerization causes the Cl–M bond to expand, and it reduces its polarity.

1. Introduction

Clusters are intermediates in the transition between gaseous and condensed phases, and their investigation provides thus valuable insight into how physicochemical properties evolve going from molecular systems to the solid state.[1] Here, we focus on table salt and other alkali metal chloride molecules and clusters $(ClM)_n$ (M = alkali metal), which occur in hot vapors of these materials.[2] Structural and thermochemical data about these species are still incomplete in spite of various pioneering experimental[2,3] and theoretical[4–9] investigations. It is known that particularly compact and stable clusters $(XM)_n$ arise for the so-called magic numbers: n = 4, 6, 9, 12, 15, and 18.[2a] These clusters exist in various isomeric forms that may be in thermal equilibrium with each other. The tetramer $(XM)_4$, for example, occurs among others as a cube (**1**), ladder (**2**), and ring (**3**);[2a] the cubic isomer (**1**) being typically (but not always) the most stable form.[4–7]

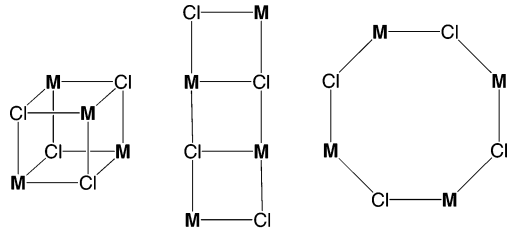

Earlier theoretical studies have shown that the cube (**1**) is the lowest-energy structure for $(ClNa)_4$ and $(ClK)_4$ followed by the ring (**3**), which is higher in energy by 5−15 kcal/mol, depending on the level of theory.[4d,6a,d,e,7b,c] For the less

* To whom correspondence should be addressed. E-mail: FM.Bickelhaupt@few.vu.nl (F.M.B.), miquel.sola@udg.es (M.S.). Fax: +31-20-59 87 629 (F.M.B.), +34-972-41 83 56 (M.S.).

† Scheikundig Laboratorium der Vrije Universiteit.

‡ Universitat de Girona.

(1) (a) Alonso, J. A. *Chem. Rev.* **2000**, *100*, 637. (b) Berry, R. S. *Chem. Rev.* **1993**, *93*, 2379.

(2) (a) Hargittai, M. *Chem. Rev.* **2000**, *100*, 2233. (b) Hargittai, M.; Hargittai, I. *The Molecular Geometries of Coordination Compounds in the Vapor Phase*; Elsevier: Amsterdam, 1997.

(3) (a) Campana, J. E.; Barlak, T. M.; Colton, R. J.; DeCorpo, J. J.; Wyatt, J. R.; Dunlap, B. I. *Phys. Rev. Lett.* **1981**, *47*, 1046. (b) Pflaum, R.; Pfau, P.; Sattler, K.; Recknagel, E. *Surf. Sci.* **1985**, *156*, 165. (c) Conover, C. W. S.; Yang, Y. A.; Bloomfield, L. A. *Phys. Rev. B* **1988**, *38*, 3517. (d) Twu, Y. T.; Conover, C. W. S.; Yang, Y. A.; Bloomfield, *Phys. Rev. B* **1990**, *42*, 5306. (e) Hebert, A. J.; Lovas, F. J.; Melendres, C. A.; Hollowell, C. D.; Story, T. L., Jr.; Street, K., Jr. *J. Chem. Phys.* **1968**, *48*, 2824. (f) Lide, D. R., Jr.; Cahill, P.; Gold, L. P. *J. Chem. Phys.* **1964**, *40*, 156. (g) Honig, A.; Mandel, M.; Stitch, M. L.; Townes, C. H. *Phys. Rev.* **1954**, *96*, 629. (h) Clouser, P.; Gordy, W. *Bull. Am. Phys. Soc.* **1963**, *8*, 326. (i) Lee, C. A.; Fabricand, B. P.; Carlson, R. O.; Rabi, I. I. *Phys. Rev.* **1953**, *91*, 1395. (j) Trischka, J. W.; Braunstein, R. *Phys. Rev.* **1954**, *96*, 968. (k) Bulewicz, E. M.; Phillips, L. F.; Sugden, T. M. *Trans. Faraday Soc.* **1961**, *57*, 921. (l) Brewer, L.; Brackett, E. *Chem. Rev.* **1961**, *61*, 425. (m) Martin, T. P. *Phys. Rep.* **1983**, *95*, 167.

10.1021/ic070328u CCC: $37.00
Published on Web 06/01/2007

polar $(ClLi)_4$ species, the cube (**1**) is disfavored with respect to the ring (**3**) but only by less than 1 kcal/mol.[7b]

The purpose of the present study is twofold. In the first place, we aim at a better understanding of the nature of highly polar chemical bonds. Previously, it was shown that the C−M and H−M bonds have substantial covalent character, i.e., stabilization deriving from bond overlap, whereas such covalence nearly disappears in the ionic F−M bond which instead gains stabilization predominantly through the electronegativity difference across the bond.[10] Here, we wish to clarify the relative importance of these covalent (bond overlap) and ionic features (electronegativity difference) in the bonding mechanism of the alkali metal chloride Cl−M bond which is of intermediate polarity between, on one hand, the C−M and H−M bonds and, on the other hand, the F−M bond. To this end, we have undertaken a detailed investigation of alkali metal chloride monomers ClM and tetramers $(ClM)_4$ with M = Li, Na, K, and Rb using the generalized gradient approximation (GGA) of density functional theory (DFT) at the BP86/TZ2P level of theory.[11,12] The polar Cl−M bonds are analyzed in the framework of the Kohn−Sham molecular orbital (KS-MO) model using a quantitative bond energy decomposition.[11]

A second objective is to obtain a set of consistent structural and thermochemical data for alkali metal chloride monomers ClM and tetramers (geometries, Cl−M bond strengths, tetramerization energies), all obtained with exactly the same GGA density functional method. This complements the available experimental and theoretical data, which are scarce, and it enables a systematic analysis of the trends. In this context, we note that experimental information on the tetramers is completely missing. For the tetramers, we focus on the cubic isomer, which is in general not a perfect but a distorted cube. In $(ClLi)_4$, for example, the lithium atoms constitute an inner cluster that is surrounded by four chlorine atoms, one on each face of the tetrahedral metal cluster (see Figure 1, left), similar to the situation for the organometallic $(CH_3Li)_4$.[10b]

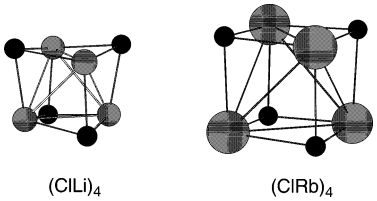

Figure 1. Structures (to scale) of alkali metal chloride tetramers for lithium and rubidium (for numerical results, see Table 1).

2. Theoretical Methods

2.1. General Procedure. All calculations were performed using the Amsterdam Density Functional (ADF) program.[12] The numerical integration was carried out using the procedure developed by Boerrigter, te Velde, and Baerends.[12e,f] The molecular orbitals (MO) were expanded in a large uncontracted set of Slater type orbitals (STOs) containing diffuse functions, which is of triple-ζ quality for all atoms and has been augmented with two sets of polarization functions: 3d and 4f on Cl, Li, and Na; 4d and 4f on K and Rb.[12g] In addition, an extra set of p functions was added to the basis sets of Li (2p), Na (3p), K (4p), and Rb (5p). The 1s core shell of lithium, the 1s2s2p core shells of chlorine, sodium, and potassium, and the 1s2s3s2p3p3d core shells of rubidium were treated by the frozen-core approximation.[12d] An auxiliary set of s, p, d, f, and g STOs was used to fit the molecular density and to represent the Coulomb and exchange-correlation potentials accurately in each SCF cycle.[12h]

Energies, geometries,[13] and frequencies[14] were computed using the generalized gradient approximation (GGA) of DFT at the BP86 level.[15] All open-shell systems were treated with the spin-unrestricted formalism.

(4) (a) Malliavin, M.-J.; Coudray, C. *J. Chem. Phys.* **1997**, *106*, 2323. (b) Häkkinen, H.; Barnett, R. N.; Landman, U. *Chem. Phys. Lett.* **1995**, *232*, 79. (c) Ochsenfeld, C.; Ahlrichs, R. *Ber. Bunsen−Ges.* **1994**, *98*, 34. (d) Weis, P.; Ochsenfeld, C.; Ahlrichs, R.; Kappes, M. M. *J. Chem. Phys.* **1992**, *97*, 2553. (e) Ahlrichs, R.; Ochsenfeld, C. *Ber. Bunsen−Ges.* **1992**, *96*, 1287. (f) Ochsenfeld, C.; Ahlrichs, R. *J. Chem. Phys.* **1992**, *97*, 3487. (g) Lintuluoto, M. *J. Mol. Struct.: THEOCHEM* **2001**, *540*, 177. (h) Lai, J.; Lu, X.; Zheng, L. *Phys. Chem. Commun.* **2002**, *5*, 82.

(5) (a) Berry, R. S.; Rose, J. *J. Chem. Phys.* **1992**, *96*, 517. (b) Heidenrich, A.; Schek, I.; Scharf, D.; Jortner, J. *Z. Phys. D* **1991**, *20*, 227. (c) Heidenrich, A.; Oref, I.; Jortner, J. *J. Phys. Chem.* **1992**, *96*, 7517. (d) Martin, T. P. *J. Chem. Phys.* **1980**, *72*, 3506.

(6) (a) Martin, T. P. *J. Chem. Phys.* **1978**, *69*, 2036. (b) Diefenbach, J.; Martin, T. P. *J. Chem. Phys.* **1985**, *83*, 4585. (c) Dunlap, B. I. *J. Chem. Phys.* **1986**, *84*, 5611. (d) Phillips, N. G.; Conover, C. W. S.; Bloomfield, L. A. *J. Chem. Phys.* **1991**, *94*, 4980. (e) Zhang, S.; Chen. N. *Physica B* **2003**, *325*, 172. (f) Diefenbach, J.; Martin, T. P. *Surf. Sci.* **1985**, *156*, 234.

(7) (a) Ayuela, A.; López, J. M.; Alonso, J. A.; Luaña, V. *Z. Phys. D* **1993**, *26*, S213. (b) Aguado, A.; Ayuela, A.; López, J. M.; Alonso, J. A. *Phys. Rev. B* **1997**, *56*, 15353. (c) Ayuela, A.; López, J. M.; Alonso, J. A.; Luaña, V. *Physica B* **1995**, *212*, 329.

(8) Törring, T.; Biermann, S.; Hoeft, J.; Mawhorter, R.; Cave, R. J.; Szemenyei, C. *J. Chem. Phys.* **1996**, *104*, 8032.

(9) (a) Langhoff, S. R.; Bauschlicher, C. W., Jr.; Partridge, H. *J. Chem. Phys.* **1986**, *84*, 1687. (b) Kim, C. K.; Won, J.; Kim, H. S.; Kang, Y. S.; Li, H. G.; Kim, C. K. *J. Comput. Chem.* **2001**, *22*, 827. (c) Mawhorter, R. J.; Fink, M.; Hartley, J. G. *J. Chem. Phys.* **1985**, *83*, 4418. (d) Dickey, R. P.; Maurice, D.; Cave, R. J. *J. Chem. Phys.* **1993**, *98*, 2182. (e) Brumer, P.; Karplus, M. *J. Chem. Phys.* **1973**, *58*, 3909.

(10) (a) Bickelhaupt, F. M.; Solà, M.; Fonseca Guerra, C. *J. Mol. Model.* **2006**, *11*, 563. (b) Bickelhaupt, F. M.; Solà, M.; Fonseca Guerra, C. *J. Chem. Theory Comput.* **2006**, *2*, 965. (c) Bickelhaupt, F. M.; Solà, M.; Fonseca Guerra, C. *Faraday Discuss.* **2007**, *135*, 451. (d) Bickelhaupt, F. M.; Solà, M.; Fonseca Guerra, C. *J. Comput. Chem.* **2007**, *28*, 238. See also, for example: (e) Jemmis, E. D.; Gopakumar, G. In *The Chemistry of Organolithium Compounds*; Rappoport, Z., Marek, I., Eds.; Wiley: New York, 2004.

(11) Bickelhaupt, F. M.; Baerends, E. J., In *Reviews in Computational Chemistry*; Lipkowitz, K. B., Boyd, D. B., Eds.; Wiley-VCH: New York, 2000; Vol. 15, pp 1−86.

(12) (a) te Velde, G.; Bickelhaupt, F. M.; Baerends, E. J.; van Gisbergen, S. J. A.; Fonseca Guerra, C.; Snijders, J. G.; Ziegler, T. *J. Comput. Chem.* **2001**, *22*, 931. (b) Fonseca Guerra, C.; Snijders, J. G.; te Velde, G.; Baerends, E. J. *Theor. Chem. Acc.* **1998**, *99*, 391. (c) Fonseca Guerra, C.; Visser, O.; Snijders, J. G.; te Velde, G.; Baerends, E. J. In *Methods and Techniques for Computational Chemistry*; Clementi, E., Corongiu, G., Eds.; STEF: Cagliari, Italy, 1995; pp 305−395. (d) Baerends, E. J.; Ellis, D. E.; Ros, P. *Chem. Phys.* **1973**, *2*, 41. (e) Boerrigter, P. M.; te Velde, G.; Baerends, E. J. *Int. J. Quantum Chem.* **1988**, *33*, 87. (f) te Velde, G.; Baerends, E. J. *J. Comp. Phys.* **1992**, *99*, 84. (g) Snijders, J. G.; Baerends, E. J.; Vernooijs, P. *At. Data Nucl. Data Tables* **1982**, *26*, 483. (h) Krijn, J.; Baerends, E. J. *Fit Functions in the HFS Method;* Internal Report; Vrije Universiteit: Amsterdam, The Netherlands, 1984 (in Dutch).

(13) (a) Versluis, L.; Ziegler. T. *J. Chem. Phys.* **1988**, *88*, 322. (b) Fan, L.; Ziegler, T. *J. Chem. Phys.* **1991**, *95*, 7401. (c) Schreckenbach, G.; Li, J.; Ziegler. T. *Int. J. Quantum Chem.* **1995**, *56*, 477.

(14) Fan, L.; Versluis, L.; Ziegler, T.; Baerends, E. J.; Ravenek. W. *Int. J. Quantum Chem. Symp.* **1988**, *22*, 173.

(15) (a) Becke, A. D. *J. Chem. Phys.* **1986**, *84*, 4524. (b) Becke, A. *Phys. Rev. A* **1988**, *38*, 3098. (c) Perdew, J. P. *Phys. Rev. B* **1986**, *33*, 8822. Erratum: Perdew, J. P. *Phys. Rev. B* **1986**, *34*, 7406. (d) Fan, L.; Ziegler, T. *J. Chem. Phys.* **1991**, *94*, 6057.

Bond enthalpies at 298.15 K and 1 atm (ΔH_{298}) were calculated from electronic bond energies (ΔE) according to eq 1, assuming an ideal gas.[16] In eq 1, $\Delta E_{trans,298}$, $\Delta E_{rot,298}$, and $\Delta E_{vib,0}$ are the

$$\Delta H_{298} = \Delta E + \Delta E_{trans,298} + \Delta E_{rot,298} + \Delta E_{vib,0} + \Delta(\Delta E_{vib,0})_{298} + \Delta(pV) \quad (1)$$

differences between products and reactants in translational, rotational, and zero point vibrational energies, respectively; $\Delta(\Delta E_{vib})_{298}$ is the change in the vibrational energy difference as one goes from 0 to 298.15 K. The vibrational energy corrections are based on our frequency calculations. The molar work term $\Delta(pV)$ is $(\Delta n)RT$ (e.g., for two fragments combining to one molecule $\Delta n = -1$). Thermal corrections for the electronic energy are neglected.

2.2. Bond Energy Decomposition. The overall bond energy ΔE is made up of two major components (eq 2). In eq 2, the preparation

$$\Delta E = \Delta E_{prep} + \Delta E_{int} \quad (2)$$

energy ΔE_{prep} is the energy needed to deform the separate molecular fragments from their equilibrium structure to the geometry that they attain in the overall molecular system. The interaction energy ΔE_{int} is the energy released when the prepared fragments are brought together into the position they have in the overall molecule. It is analyzed for our model systems in the framework of the KS-MO model using a Morokuma-type decomposition into electrostatic interaction, Pauli repulsion (or exchange repulsion), and (attractive) orbital interactions (eq 3).[11,17] The term ΔV_{elst} corresponds to the

$$\Delta E_{int} = \Delta V_{elst} + \Delta E_{Pauli} + \Delta E_{oi} \quad (3)$$

classical electrostatic interaction between the unperturbed charge distributions of the prepared (i.e., deformed) fragments and is usually attractive. The Pauli-repulsion, ΔE_{Pauli}, comprises the destabilizing interactions between occupied orbitals and is responsible for the steric repulsion. The orbital interaction ΔE_{oi} in any MO model, and therefore also in Kohn−Sham theory, accounts for electron-pair bonding, charge transfer (i.e., donor−acceptor interactions between occupied orbitals on one fragment with unoccupied orbitals of the other, including the HOMO−LUMO interactions), and polarization (empty−occupied orbital mixing on one fragment due to the presence of another fragment). In the case of open-shell fragments, the bond energy analysis yields, for technical reasons, interaction energies that differ consistently on the order of a kcal/mol from the exact BP86 result. To facilitate a straightforward comparison, the results of the bond energy analysis were scaled to match exactly the regular BP86 bond energies.

The orbital interaction energy can be decomposed into the contributions from each irreducible representation Γ of the interacting system (eq 4) using the extended transition state (ETS) scheme developed by Ziegler and Rauk.[17d,e]

$$\Delta E_{oi} = \sum_{\Gamma} \Delta E_{\Gamma} \quad (4)$$

2.3. Analysis of the Charge Distribution. The electron density distribution is analyzed using the Voronoi deformation density (VDD) method[18,19] and the Hirshfeld scheme[20] for computing atomic charges. The VDD atomic charge Q_A^{VDD} is computed as the (numerical) integral[12f] of the deformation density $\Delta\rho(\mathbf{r}) = \rho(\mathbf{r}) - \sum_B \rho_B(\mathbf{r})$ in the volume of the Voronoi cell of atom A (eq 5). The Voronoi cell of atom A is defined as the compartment of space bound by the bond midplanes on and perpendicular to all bond axes between nucleus A and its neighboring nuclei (cf. the Wigner−Seitz cells in crystals).[19c] In eq 5, $\rho(\mathbf{r})$ is the electron density of the

$$Q_A^{VDD} = -\int_{\text{Voronoi cell of A}} (\rho(\mathbf{r}) - \sum\nolimits_B \rho_B(\mathbf{r}))\mathrm{d}\mathbf{r} \quad (5)$$

molecule and $\sum_B \rho_B(\mathbf{r})$ the superposition of atomic densities ρ_B of a fictitious promolecule without chemical interactions that is associated with the situation in which all atoms are neutral. The interpretation of the VDD charge Q_A^{VDD} is rather straightforward and transparent. Instead of the measurement of the amount of charge associated with a particular atom A, Q_A^{VDD} directly monitors how much charge flows, due to chemical interactions, out of ($Q_A^{VDD} > 0$) or into ($Q_A^{VDD} < 0$) the Voronoi cell of atom A, that is, the region of space that is closer to nucleus A than to any other nucleus.

3. Results and Discussion

3.1. Structures. 3.1.a. Monomers. The computed BP86/TZ2P geometries are summarized in Table 1 and Figure 1. The Cl−M bond distance in the diatomic alkali metal chloride monomers increases systematically from 2.077 to 2.434 to 2.769 to 2.878 Å along M = Li, Na, K, and Rb, respectively. Note that the increase in bond length in every step becomes smaller as one descends the periodic table.

This trend agrees well with earlier theoretical work[4a−c,f,8,9a,b,d] and microwave and electron diffraction (ED) experiments,[3f−j,9c] which also yield a monotonic increase of the Cl−M bond along ClLi, ClNa, ClK, and ClRb. The experimental bond lengths are however systematically shorter by 2−4% than our BP86/TZ2P and most other theoretical values. The CI-(SD) bond lengths of Langhoff et al.[9a] are somewhat closer to our BP86/TZ2P results with values that are smaller by 2−3%.

3.1.b. Tetramers. Tetramerization causes the Cl−M bond to expand by approximately 0.29 Å for all the alkali metals studied (see Table 1). Thus, the Cl−M bond in the T_d symmetric alkali metal chloride tetramers increases monotonically if one descends the periodic table from 2.369 (Li) to 2.727 (Na) to 3.046 (K) to 3.163 Å (Rb), similar to the monomers but at somewhat larger values than in the latter. The chloride tetrahedron is larger than the metal cluster for all four alkali metals studied (i.e., Cl−Cl > M−M; see Figure 1). This is similar to the situation for the corresponding methylalkali metal tetramers.[10a,b] However, it differs strikingly from the situation for alkali metal fluorides.[10d] In the case of the latter, the F_4 is also larger than the M_4 cluster

(16) Atkins, P. W. *Physical Chemistry*; Oxford University Press: Oxford, U.K., 1982.
(17) (a) Morokuma, K. *J. Chem. Phys.* **1971**, *55*, 1236. (b) Kitaura, K.; Morokuma, K. *Int. J. Quantum. Chem.* **1976**, *10*, 325. (c) Bickelhaupt, F. M.; Nibbering, N. M. M.; van Wezenbeek, E. M.; Baerends, E. J. *J. Phys. Chem.* **1992**, *96*, 4864. (d) Ziegler, T.; Rauk, A. *Inorg. Chem.* **1979**, *18*, 1558. (e) Ziegler, T.; Rauk, A. *Theor. Chim. Acta* **1977**, *46*, 1.
(18) Bickelhaupt, F. M.; van Eikema Hommes, N. J. R.; Fonseca Guerra, C.; Baerends, E. J. *Organometallics* **1996**, *15*, 2923.
(19) See also: (a) Fonseca Guerra, C.; Bickelhaupt, F. M.; Snijders, J. G.; Baerends, E. J. *Chem.—Eur. J* **1999**, *5*, 3581. (b) Fonseca Guerra, C.; Handgraaf, J. W.; Baerends, E. J.; Bickelhaupt, F. M. *J. Comput. Chem.* **2004**, *25*, 189. Voronoi cells are equivalent to Wigner−Seitz cells in crystals; for the latter, see: (c) Kittel, C. *Introduction to Solid State Physics*; Wiley: New York, 1986.
(20) Hirshfeld, F. L. *Theor. Chim. Acta* **1977**, *44*, 129.
(21) Mann, J. B.; Meek, T. L.; Allen, L. C. *J. Am. Chem. Soc.* **2000**, *122*, 2780.

Table 1. Structures (in Å) of Alkali Metal Chloride Monomers and Tetramers

system	method	Cl−M	M−M	Cl−Cl	ref
ClLi	BP86/TZ2P	2.077			this work
	HF	2.036			9a
	B3LYP/6-311+G*	2.024			9b
	B3LYP/6-311+G(2df,p)	2.023			9b
	MP2/6-311+G*	2.023			9b
	MP2/6-311+G(2df,p)	2.037			9b
	CI(SD)	2.033			9a
	exptl: microwave[a]	2.02067(6)			3f
$(ClLi)_4$	BP86/TZ2P	2.369	2.922	3.690	this work
ClNa	BP86/TZ2P	2.434			this work
	HF	2.389			4f
	HF	2.389			9a
	VWN	2.386			4b
	LDA	2.33			4a
	B3LYP/6-311+G*	2.383			9b
	B3LYP/6-311+G(2df,p)	2.375			9b
	MP2/6-31G+pol	2.384			9d
	CI(SD)	2.366			9a
	exptl: microwave[a]	2.3606(1)			3g,h
	exptl: microwave[a]	2.3609			9c
	exptl: electron diffraction[a]	2.359(8)			9c
	exptl: electron diffraction[a]	2.388(8)			9c
$(ClNa)_4$	BP86/TZ2P	2.727	3.545	4.123	this work
	HF	2.680	*b*	*b*	4f
	VWN	2.640	*b*	*b*	4b
	LDA	2.58	*b*	*b*	4a
	MP2	2.624	*b*	*b*	4f
ClK	BP86/TZ2P	2.769			this work
	HF	2.739			9a
	B3LYP/6-311+G*	2.698			9b
	B3LYP/6-311+G(2df,p)	2.698			9b
	MP2/ECP	2.690			8
	CI(SD)	2.697			9a
	CCSD(T)	2.678			9c
	exptl: microwave[a]	2.6666(1)			3h,i
	exptl: microwave[a]	2.6668			9c
	exptl: electron diffraction[a]	2.669(8)			9c
	exptl: electron diffraction[a]	2.703(8)			9c
$(ClK)_4$	BP86/TZ2P	3.046	4.167	4.439	this work
	HF	3.079	*b*	*b*	9c
	MP2	2.961	*b*	*b*	9c
ClRb	BP86/TZ2P	2.878			this work
	HF	2.876			9a
	MP2/ECP	2.799			8
	CI(SD)	2.829			9a
	exptl: microwave[a]	2.78670(6)			3j
	exptl: microwave[a]	2.7869			9c
	exptl: electron diffraction[a]	2.784(4)			9c
	exptl: electron diffraction[a]	2.817(4)			9c
$(ClRb)_4$	BP86/TZ2P	3.163	4.336	4.603	this work

[a] Represents r_e values. [b] Not specified in reference.

for Li and Na (i.e., F−F > M−M); however, it is *smaller* than and inside the M_4 cluster for the heavier alkali metals K and Rb (i.e., F−F < M−M). Likewise, the corresponding alkali metal hydrides have the H_4 outside a central M_4 core for M = Li and Na (i.e., H−H > M−M), but it is inside the M_4 cluster for the large M = K and Rb (i.e., H−H < M−M).[10c] This difference in the behavior along Li−Rb between the alkali metal chloride and the methyl alkali metal tetramers, on one hand, and the alkali metal fluorides and hydrides, on the other hand, suggests a larger steric demand of a Cl or CH_3 group as compared to F and H.

We are not aware of any experimental data on the geometry parameters of alkali metal chloride tetramers. This prevents a comparison of structural trends found by us with experiment. Other theoretical work[4c,f] is also limited to Hartree−Fock and MP2 geometries for $(ClNa)_4$ and $(ClK)_4$ and two LDA geometries for $(ClNa)_4$. The trends that evolve from both the Hartree−Fock and MP2 $(ClM)_4$ structures agree with ours; i.e., the Cl−M bond elongates from Na to K, and for both metals, the M_4 cluster is smaller than and surrounded by the Cl_4 tetrahedron ∠M−Cl−M < 90° (not shown in Table 1).

3.2. Thermochemistry. 3.2.a. Monomers. The thermochemical results of our BP86/TZ2P calculations are collected in Tables 2 (monomers) and 3 (tetramers). Homolytic dissociation of the Cl−M bond in alkali metal chloride monomers (i.e., $ClM \rightarrow Cl^{\bullet} + M^{\bullet}$) is favored over heterolytic or ionic dissociation (i.e., $ClM \rightarrow Cl^{-} + M^{+}$) for all alkali metal chloride monomers with heterolytic bond dissociation enthalpies (BDE = $-\Delta H$ in Table 2) being 1.2−1.5 times higher than the homolytic ones. This is because charge separation is energetically highly unfavorable in the gas phase. The Cl−M bond strength decreases markedly if one goes from lithium to the heavier alkali metals and is more or less constant along the latter. For example, the homolytic BDE is −105.2, −90.4, −93.9, and −93.6 kcal/mol when M = Li, Na, K, and Rb (see ΔH_{homo} in Table 2).

The results of our BP86/TZ2P computations agree well with those of experimental and other theoretical studies, which all find a sizable decrease in homolytic bond strength going from Li to Na followed by only slight changes along Na−Rb (see Table 2). For example, the homolytic bond dissociation energies ΔE_{homo} at CI(SD) are −111.2, −97.1, −99.4, and −98.7 kcal/ mol with Li, Na, K, and Rb as compared to −105.2, −90.2, −93.7, and −93.3 kcal/mol at BP86/TZ2P. The corresponding experimental thermochemical D_0 values are −111.8, −97.5, −101.2, and −100.8 kcal/mol.

3.2.b. Tetramers. The tetramerization enthalpies of the alkali metal chlorides (i.e., ΔH_{tetra} associated with the reaction $4ClM \rightarrow (ClM)_4$, see Table 3) become systematically less stabilizing if one descends the periodic table, i.e., from −134.1 (Li) to −123.7 (Na) to −120.2 (K) to −116.0 kcal/mol (Rb). These tetramerization enthalpies are all significantly more stabilizing than the corresponding values for methyl alkali metal molecules CH_3M (ΔH_{tetra} = −120.3, −73.5, −82.5, and −87.1 kcal/mol for Li, Na, K, and Rb)[10b] and less stabilizing than those of alkali metal fluorides FM (ΔH_{tetra} = −169.1, −156.1, −144.8, and −135.8 kcal/mol).[10c] The tetramerization energy decreases much more pronouncedly going from Li to Na in the case of the methyl alkali metals than for alkali metal fluorides and chlorides.

There are no experimental tetramerization energies for alkali metal chlorides, and theoretical data[4b,c,d,h] are provided only for sodium and potassium chloride (see Table 3). Thus, only a limited comparison can be performed between the trends we find along Li−Rb with those of other theoretical studies along Na and K. The HF and MP2 values[4d] of −139.7 and −151.4 kcal/mol for Na and K for the tetramerization energy ΔE_{tetra} are 14 and 25 kcal/mol more stabilizing than the BP86/TZ2P value. Note that the MP2 value is even more stabilizing than the one obtained at VWN, which is known to cause overbinding. This comparison suggests that our approach may somewhat underestimate and the ab initio

Table 2. Homolytic and Heterolytic Cl−M Bond Strength (in kcal/mol) of Alkali Metal Chloride Monomers

		bond energies[b]		bond enthalpies[c]		
monomer	method[a]	ΔE_{homo}	ΔE_{hetero}	ΔH_{homo}	ΔH_{hetero}	ref
ClLi	BP86/TZ2P	−105.2	−150.8	−105.2	−150.8	this work
	HF	−110.5				9a
	B3LYP/6-311+G*		−153.0			9b
	B3LYP/6-311+G(2df,p)		−154.2			9b
	MP2/6-311+G*		−155.6			9b
	MP2/6-311+G(2df,p)		−153.9			9b
	CI(SD)	−111.2				9a
	exptl: flame photometry[d]	−110.5 ± 3.0				3k
	exptl: thermochemical[d]	−111.8				3l
	exptl[d]		−152.0			9b
	exptl[d]		−153.3			9e
ClNa	BP86/TZ2P	−90.2	−131.1	−90.4	−131.3	this work
	HF	−94.1				9a
	HF		−135.1			4g
	B3LYP/6-311+G*		−131.2			9b
	B3LYP/6-311+G(2df,p)		−132.6			9b
	MP2		−154.0			4g
	CI(SD)	−97.1				9a
	exptl: flame photometry[d]	−97.5 ± 2.1				3k
	exptl: thermochemical[d]	−97.5				3l
	exptl[d]		−132.6			9b
	exptl[d]		−132.6			9e
ClK	BP86/TZ2P	−93.7	−114.2	−93.9	−114.4	this work
	HF	−95.7				9a
	B3LYP/6-311+G*		−114.7			9b
	B3LYP/6-311+G(2df,p)		−115.7			9b
	CI(SD)	−99.4				9a
	exptl: flame photometry[d]	−99.6 ± 2.1				3k
	exptl: thermochemical[d]	−101.2				3l
	exptl[d]		−117.8			9b
	exptl[d]		−118.0			9e
ClRb	BP86/TZ2P	−93.3	−109.0	−93.6	−109.3	this work
	HF	−94.5				9a
	CI(SD)	−98.7				9a
	exptl: flame photometry[d]	−101.5 ± 2.1				3k
	exptl: thermochemical	−100.8				3l
	exptl[d]		−113.4			9e

[a] Energy and structure obtained at the same level of theory. [b] Electronic energies at 0 K. [c] Enthalpies at 298.15 K. [d] D_o values. ZPE for ClLi, ClNa, ClK, and ClRb are calculated to be 0.9, 0.5, 0.4, and 0.3 kcal/mol, respectively, at BP86/T2ZP.

Table 3. Tetramerization Energies and Enthalpies (in kcal/mol) of Alkali Metal Chloride Monomers

monomer	method[a]	ΔE_{tetra}[b]	ΔH_{tetra}[c]	ref
ClLi	BP86/TZ2P	−136.6	−134.1	this work
ClNa	BP86/TZ2P	−126.1	−123.7	this work
	HF/tzp	−139.7		4d
	HF/CEP-31G*	−146.9		4h
	VWN/pw[d]	−144.3		4b
	BP86//VWN/pw[d]	−136.5		4b
	B3LYP/CEP-31G*	−134.4		4h
	MP2/tzp	−151.4		4d
ClK	BP86/TZ2P	−122.4	−120.2	this work
	MP2	−142.9		4c
ClRb	BP86/TZ2P	−118.5	−116.0	this work

[a] Energy and structure obtained at the same level of theory. [b] Electronic energies at 0 K. [c] Enthalpies at 298.15 K. [d] Plane wave basis with kinetic-energy cutoff of $E_c = 20.1$ Ry.

computations overestimate the tetramerization energies. The trend in MP2 values[4c,d] of ΔE_{tetra} along Na and K agrees with ours; i.e., the tetramerization energy decreases if one goes to the heavier alkali metal.

3.3. Analysis of the Cl−M Bond in Alkali Metal Chloride Monomers. 3.3.a. Orbital Mixing. The electronic structure analyses of the alkali metal chlorides confirm the high polarity in combination with a predominantly ionic Cl−M bonding mechanism. They reveal however also a decrease in polarity and an increase in covalent contributions to the bonding if compared to the F−M bond.[10d] Still, however, the nature of the Cl−M bond resembles more closely that of the F−M bond[10d] than that of the more covalent C−M and H−M bonds.[10a−c] In the first place, for all four alkali metals, the Cl−M bond is characterized by a rather weak mixing between the chlorine $3p_\sigma$ AO and the alkali metal *n*s AO in the $3p_\sigma$ + *n*s electron-pair bonding MO. In terms of Gross Mulliken contributions,[22] the latter is approximately 93% $3p_\sigma$ + 4% *n*s (see Figure 2). This strong polarization toward the halide atom is essentially the same as that in the F−M bonds,[10d] whereas the corresponding methyl alkali metal C−M bonds are significantly less polarized toward the methyl fragment (approximately 70% $2a_1$ + 25% *n*s).[10a,b]

3.3.b. Charge Distribution. Second, the metal atomic charge in ClM increases along Li, Na, and K and, only slightly so, from K to Rb according to both the VDD and Hirshfeld method (see Table 4). The VDD method, for example, yields values of +0.500, +0.590, +0.642, and +0.662 e along the

(22) The description of the MO in terms of fragment MO coefficients instead of Gross Mulliken contributions yields the same picture, but it has the disadvantage of not being normalized; that is, the figures do not add up to 1 (or to 100%).

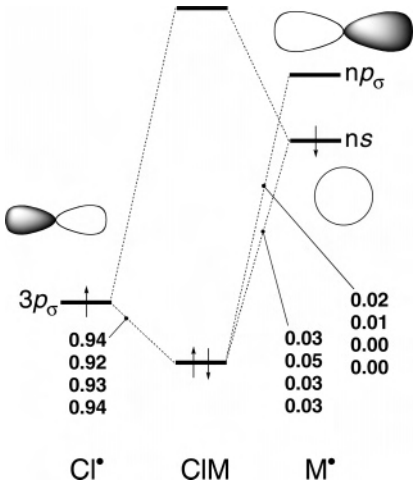

Figure 2. Orbital interaction diagram for ClM with Gross Mulliken contributions at BP86/TZ2P of the Cl• and M• fragment orbitals to the Cl−M electron-pair bonding MO for M = Li, Na, K, and Rb.

Table 4. Metal Atomic Charge (in e) and Dipole Moment μ (in D) of Alkali Metal Chloride Monomers and Tetramers[a]

	ClLi	ClNa	ClK	ClRb	$(ClLi)_4$	$(ClNa)_4$	$(ClK)_4$	$(ClRb)_4$
VDD	0.500	0.590	0.642	0.662	0.289	0.422	0.459	0.458
Hirshfeld	0.527	0.579	0.639	0.646	0.303	0.404	0.467	0.477
μ	7.197[b]	8.943[c]	10.788[d]	11.207[e]	0	0	0	0

[a] At BP86/TZ2P. Experimental dipole moments from ref 3e. [b] Experimental: 7.1289(10) D. [c] Experimental: 9.0020(5) D. [d] Experimental: 10.2688(10) D. [e] Experimental: 10.510(5) D.

series Li, Na, K, and Rb. In agreement with this and the increasing Cl−M bond length, the dipole moment μ increases steeply at first and then more moderately: μ = 7.2, 8.9, 10.8, and 11.2 D along Li, Na, K, and Rb (Table 4). These Cl−M dipole moments are somewhat larger than those of the corresponding F−M bonds (6.511, 8.293, 9.510, and 9.877 D, respectively, along Li, Na, K, and Rb).[10d] The main reason for the larger dipole moments in alkali metal chlorides is the longer distance in Cl−M than F−M bonds and not a larger atomic charge.

3.3.c. Bond Energy Decomposition. Third, in line with the weak Cl−M mixing, the covalent stabilization due to $3p_\sigma + ns$ overlap is much smaller than the ionic stabilization received from the dropping of the metal *n*s electron into the chloride $3p_\sigma$. The ionic stabilization is related to the electronegativity difference $\Delta\chi$ indicated in **4**. It is equal to

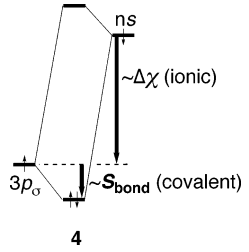

4

the difference in orbital energies $\epsilon(3p_\sigma) - \epsilon(ns)$ which, for Cl−M bonds, amounts to −156.8 (Li), −161.4 (Na), −170.6 (K), and −175.3 kcal/mol (Rb) (see Table 5 and Figure 3). The reason why the Cl−M bond is weaker than the F−M bond[10d] is that this ionic term in the orbital interactions

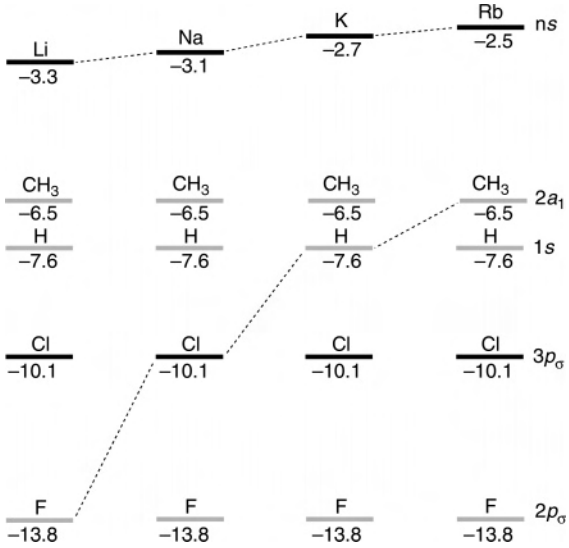

Figure 3. Energies (in eV) of the SOMOs of alkali metal, chlorine, fluorine, hydrogen, and methyl (in the geometry it adopts in CH_3Li) radicals, computed at BP86/TZ2P.

Table 5. Analysis of the Cl−M Bond between Cl• and M• in Alkali Metal Chloride Monomers[a]

	Cl−Li	Cl−Na	Cl−K	Cl−Rb
Bond Energy Decomposition (in kcal/mol)				
ΔE_σ	−126.2	−103.7	−105.1	−105.2
ΔE_π	−4.0	−1.6	−1.6	−1.5
ΔE_{oi}	−130.2	−105.3	−106.7	−106.7
ΔE_{Pauli}	54.1	37.0	30.6	30.8
ΔV_{elstat}	−29.1	−21.9	−17.6	−17.4
$\Delta E_{int} = \Delta E$	−105.2	−90.2	−93.7	−93.3
Fragment Orbital Overlap $\langle Cl\|M\rangle$[b]				
$\langle 3s\|ns\rangle$	0.32	0.26	0.23	0.22
$\langle 3p_\sigma\|ns\rangle$	0.20	0.18	0.13	0.12
$\langle 3p_\pi\|np_\pi\rangle$	0.26	0.21	0.17	0.16
Fragment Orbital Energy Difference and Interaction Matrix Element $\langle Cl\|F\|M\rangle$ (in kcal/mol)[b,c]				
$\langle 3p_\sigma\|F\|ns\rangle$	−44.9	−40.5	−26.4	*c*
$\langle 3p_\sigma\|F\|ns\rangle^2/[\epsilon(3p_\sigma) - \epsilon(ns)]$	−12.9	−10.2	−4.1	*c*
$2\langle 3p_\sigma\|F\|ns\rangle^2/[\epsilon(3p_\sigma) - \epsilon(ns)]$	−25.8	−20.4	−8.2	*c*
$\epsilon(3p_\sigma) - \epsilon(ns)$	−156.8	−161.4	−170.6	−175.3
sum	−182.6	−181.8	−178.8	
Fragment Orbital Population (in Electrons)				
Cl				
$3p_\sigma$	1.88	1.84	1.87	1.89
$3p_\pi$	1.90	1.91	1.91	1.90
M				
ns^b	0.06	0.11	0.07	0.06
$np_\pi{}^b$	0.07	0.04	0.02	0.02

[a] At BP86/TZ2P. See section 2.2 for explanation of energy terms. [b] With *n* = 2, 3, 4, and 5 for M = Li, Na, K, and Rb, respectively. [c] Computed with the fully converged SCF density of ClM. Cannot yet be computed for Rb, for technical reasons.

becomes less stabilizing in the former bond due to the smaller difference in orbital energies or, in other words, because of the smaller Cl−M than F−M electronegativity difference (see Figure 3).

The covalent bond overlap-derived stabilization (see S_{bond} in **4**) of our electron-pair bonding $3p_\sigma + ns$ combination with respect to $\epsilon(3p_\sigma)$ is, in second order (and neglecting the effect of other occupied and virtual orbitals), given by $\langle 3p_\sigma|F|ns\rangle^2/\epsilon(3p_\sigma) - \epsilon(ns)$, that is, the interaction-matrix element squared

and divided by the difference in orbital energies.[23] The Cl−M bond interaction-matrix elements $F_{bond} = \langle 3p_\sigma|F|ns\rangle$ between the two SOMOs decrease from −44.9 to −40.5 to −26.4 kcal/mol along M = Li, Na, and K (see Table 5; *F* is the effective one-electron Hamiltonian or Fock operator evaluated with the fully converged SCF density of the molecule). These F_{bond} values are somewhat larger than those for the corresponding F−M bonds [i.e., −27.4 (Li) to −27.4 (Na) to −15.3 kcal/mol (K)][10d] but still smaller than those of the corresponding C−M bonds in methyl alkali metal molecules [i.e., −66.5 (Li), −60.9 (Na), and −43.7 kcal/mol (K)].[10a,b] The trend in F_{bond} values is directly related to the same trend in Cl−M bond overlap integrals S_{bond} which decrease from Cl−Li to Cl−Rb (see Table 5) as the metal *n*s AOs becomes more diffuse and extended along this series, leading to a smaller optimum overlap at a longer equilibrium bond distance.[24] Thus, the additional Cl−M bond overlap-derived stabilization for the two electrons in $3p_\sigma + ns$, that is, 2 times $\langle 3p_\sigma|F|ns\rangle^2/[\epsilon(2p_\sigma) - \epsilon(ns)]$, amounts to −25.8, −20.4, and −8.2 kcal/mol along M = Li, Na, and K (see Table 5).

The sum of these estimations of ionic and covalent stabilization, i.e., $\epsilon(3p_\sigma) - \epsilon(ns) + 2\langle 3p_\sigma|F|ns\rangle^2/\epsilon(2p_\sigma) - \epsilon(ns)$, is nearly constant, namely, −182.6, −181.8, and −178.8 kcal/mol along M = Li, Na, and K (see Table 5). This has to be compared with the orbital interactions ΔE_{oi} from our quantitative bond energy decomposition (see Table 5). They are smaller and show a large decrease from Li (−130.2 kcal/mol) to Na (−105.3 kcal/mol) and are practically constant, thereafter, along Na−Rb. This trend in ΔE_{oi} is also conserved in the trend in overall bond strength ΔE (see Table 5). The relatively constant value of the bond energy and orbital interactions along Cl−Na, Cl−K, and Cl−Rb is in line with the correspondingly small and counteracting changes in the basic bonding parameters discussed above.

The pronounced decrease of orbital interactions ΔE_{oi} (and thus the bond strength ΔE_{homo}) from Cl−Li to Cl−Na may be partially ascribed to the loss of the small, stabilizing contribution of the lithium $2p_\sigma$ AO (see Figure 3). However, the main reason is probably the drastic reorganization in the charge distribution as this highly polar bond is formed from two neutral atoms. This phenomenon, which is normally left out in qualitative MO considerations, causes a destabilization of the bonding electron-pair as each of the two electrons go from an initially neutral atom (Cl and M) to a situation in which they occupy the $3p_\sigma$ AO in a strongly anionic chlorine atom. This destabilization is balanced by the proximity of the strongly positively charged metal atom which stabilizes the excess negative charge on chlorine. This stabilization is most effective, leading to the strongest orbital interactions, for the positively charged lithium because this atom is most compact and approaches most closely the negatively charged chlorine atom. Unfortunately, the above "charge effect" on ΔE_{oi} cannot be straightforwardly quantified.

Table 6. Monomer−Monomer Bond Energy (in kcal/mol) Decomposition for Alkali Metal Chloride Tetramers[a]

	$(ClLi)_4$	$(ClNa)_4$	$(ClK)_4$	$(ClRb)_4$
ΔE_{oi}	−66.3	−41.7	−34.5	−35.3
ΔE_{Pauli}	116.5	86.4	85.3	98.6
ΔV_{elstat}	−207.4	−187.1	−184.2	−189.9
ΔE_{int}	−157.2	−142.4	−133.4	−126.6
ΔE_{prep}	20.6	16.3	11.0	8.1
ΔE_{tetra}	−136.6	−126.1	−122.4	−118.5

[a] At BP86/TZ2P.

Heterolytic Bond Dissociation. Finally, another criterion for classifying the Cl−M bond as mainly ionic is the reduced intrinsic preference for dissociating homolytically as compared to dissociating heterolytically (vide supra). To enable a quantitative comparison with other bonds, we have computed the ratio of $\Delta E_{hetero}/\Delta E_{homo}$ as a measure for this preference using bond energy values from Table 2. The $\Delta E_{hetero}/\Delta E_{homo}$ ratios of ClLi, ClNa, ClK, and ClRb are 1.4, 1.5, 1.2, and 1.2, respectively. These values are essentially equal to those for the corresponding F−M bonds (1.4, 1.4, 1.2, and 1.2 for FLi, FNa, FK, and FRb),[10d] but they are significantly smaller than the $\Delta E_{hetero}/\Delta E_{homo}$ ratios of the corresponding C−M bonds of the methyl alkali metal monomers (3.9, 5.0, 4.9, and 5.0 for C−Li, C−Na, C−K, C−Rb)[10b] and that of the C−H bond in methane (3.8) which is in general considered a classical covalent bond.[10b] Thus, the Cl−M bond behaves, just as the F−M bond, clearly more ionic than the C−M bond (and the C−H bond) also in the sense that heterolytic dissociation (as compared to homolytic dissociation) has become energetically much less unfavorable. In this context, it is also interesting to note that our analyses do confirm the classical picture that the heterolytically dissociating Cl−M bond becomes weaker along M = Li, Na, K, and Rb because of an increasing bond distance and thus weaker electrostatic attraction between the Cl^- and M^+ point charges (not shown in Table 5; values for C−M, H−M, and F−M bonds can be found in refs 10b−d).

In conclusion, the Cl−M bond is not only highly polar in terms of its charge distribution, it is also mainly provided by the ionic bonding mechanism associated with the metal electron dropping into the chlorine $3p_\sigma$ SOMO. Bond-overlap derived stabilization plays a smaller role although it has been found to be larger than in the corresponding F−M bonds.

3.4. Analysis of Monomer−Monomer Interaction in ClM Tetramers. To understand the stability of the alkali metal chloride tetramers toward dissociation into the four monomers, we have analyzed the interaction between these monomers in the tetramer. The decomposition of the tetramerization energy, shown in Table 6, reveals that the electrostatic attraction ΔV_{elstat} is the dominant bonding force. This term decreases from −207.4 (ClLi) to −187.1 kcal/mol (ClNa) and then more moderately to −184.2 kcal/mol (ClK); thereafter it increases slightly to −189.9 kcal/mol (ClRb). This correlates well with the Cl−M bond length,

(23) Albright, T. A.; Burdett, J. K.; Whangbo, M. *Orbital Interactions in Chemistry*; Wiley: New York, 1985.

(24) The Cl−M bond distance also increases along Li−Rb because of the increasing number of metal core shells that enter into Pauli repulsion with closed shells on the methyl fragment. For a discussion on how the interplay of bonding and repulsive orbital interactions determines bond lengths, see for examples: (a) Bickelhaupt, F. M.; DeKock, R. L.; Baerends, E. J. *J. Am. Chem. Soc.* **2002**, *124*, 1500. (b) Bickelhaupt, F. M.; Baerends, E. J. *Angew. Chem., Int. Ed.* **2003**, *115*, 4315. Bickelhaupt, F. M.; Baerends, E. J. *Angew. Chem., Int. Ed.* **2003**, *42*, 4183.

which increases more strongly from Li to K causing the electrostatic interactions to become weaker. From K to Rb, the Cl−M bond expands only slightly (from 2.769 to 2.878 Å, see Table 1) and the increase in charge separation eventually causes a slight increase in ΔV_{elstat}.

The orbital interactions ΔE_{oi} between the ClM monomers, although much smaller than ΔV_{elstat}, are still important for the cohesion between the monomers, with values ranging from −66.3 kcal/mol for the lithium chloride tetramer to −34.5 kcal/mol for the potassium chloride tetramer (Table 6). Note that these orbital interactions do not involve the formation of an electron-pair bond. They are mainly provided by donor−acceptor interactions of occupied σ_{Cl-M} and Cl lone-pair orbitals (mainly located on Cl) with unoccupied σ^*_{Cl-M} orbitals (mainly located on M) of the monomers. Consequently, tetramerization reduces the charge separation because the donor−acceptor orbital interactions cause charge transfer from Cl to M. This is also confirmed by the VDD and Hirshfeld atomic charges, which are consistently smaller in $(ClM)_4$ than in ClM (see Table 4). The same phenomenon has also been observed for the corresponding alkali metal fluorides, hydrides, and methyl alkali metal systems.[10b−d] The net interaction energy ΔE_{int} between ClM monomers decreases steadily from −157.2 to −126.6 kcal/mol along Li−Rb. This trend is preserved in the overall tetramerization energies and enthalpies (see Tables 3 and 6).

4. Conclusions

The Cl−M bond in table salt and other alkali metal chlorides not only is highly polar (e.g., significantly more so than the corresponding C−M bonds in methyl alkali metal oligomers) but also is ionic in terms of its bonding mechanism: the stabilization associated with the Cl−M bond is predominantly caused by the transfer of an electron from a high-energy SOMO on the electropositive M to a low-energy SOMO on Cl. The covalent term in the bonding mechanism, that is, the stabilization that derives from the Cl−M bond overlap, is much less important, although it is clearly larger than in the F−M bonds. Furthermore, the fact that the Cl−M bonds are weaker than the corresponding F−M bonds but stronger than the corresponding C−M bonds is entirely determined by the trend in the ionic bonding term, i.e., the trend in electronegativity difference across the metal−element bond which decreases along F−M > Cl−M > C−M. The origin of the larger dipole moments in alkali metal chlorides than fluorides is the longer Cl−M bond and not a more strongly polarized bond orbital. Finally, tetramerization causes the Cl−M bond to expand, and it reduces its polarity.

Acknowledgment. We thank the following organizations for financial support: the HPC-Europa and the TMR programs of the European Union, The Netherlands Organization for Scientific Research (NWO-CW), the Ministerio de Educación y Ciencia (MEC, Project No. CTQ 2005-08797-C02-01), the DURSI (Generalitat de Catalunya, Project No. SGR2005-00238), and the National Research School Combination-Catalysis (NRSC-C). Excellent service by the Stichting Academisch Rekencentrum Amsterdam (SARA) and the Centre de Supercomputació de Catalunya (CESCA) is gratefully acknowledged.

IC070328U